J. Plasma Physics (2013), vol. 79, part 5, pp. 577–585. © Cambridge University Press 2013
doi:10.1017/S002237781300007X

Higher harmonics generation by a spiraling ion beam in collisionless magnetized plasma

JYOTSNA SHARMA[1], SURESH C. SHARMA[2], V. K. JAIN[1] and AJAY GAHLOT[3]

[1]Physics Group, School of Environmental Sciences, Jawaharlal Nehru University, New Delhi-110066, India
[2]Department of Applied Physics, Delhi Technological University, Shahbad Daulatpur, Bawana Road, Delhi-110042, India (suresh321sharma@gmail.com)
[3]Department of Physics, Maharaja Surajmal Institute of Technology, C-4, Janakpuri, New Delhi, India

(Received 2 September 2012; revised 26 November 2012; accepted 7 January 2013; first published online 11 February 2013)

Abstract. A spiraling ion beam propagating through a magnetized plasma cylinder containing K^+ light positive ions, electrons, and $C_7F_{14}^-$ heavy negative ions drives electrostatic ion–cyclotron waves to instability via cyclotron interaction. Higher harmonics of the beam cyclotron frequency can be generated in this way. The unstable mode frequencies and growth rates of both unstable light positive ions and heavy negative ions increase with the relative density of heavy negative ions. Moreover, the growth rate of unstable modes scales as the one-third power of the beam density. The growth rate of unstable modes increases with harmonic number. The frequencies of both unstable modes also increase with magnetic fields. In addition, the real part of both unstable modes (K^+ and $C_7F_{14}^-$) increases with the beam energy and scales as almost one-half power of the beam energy.

1. Introduction

The electrostatic ion–cyclotron (EIC) instability is a low-frequency, field-aligned current-driven instability that has one of the lowest threshold drift velocities among current-driven instabilities. These waves are observed in a wide variety of situations, ranging from laboratory experiments (D'Angelo and Motley 1962; Motley and D'Angelo 1963) to space plasmas (D'Angelo 1973; Bergman 1984). The first experimental observations of EIC oscillations in laboratory plasmas were reported by D'Angelo and Motely (1962). The observed oscillations were identified as the current-driven EIC instability, which had been theoretically predicted by Drummond and Rosenbluth (1962). Ishizuka et al. (1974) observed the excitation of ion–cyclotron waves due to ion beam. The experiment was performed in pulsed helium plasma, in which a high-energy ion beam of several kiloelectron volts energy was injected. Michelson et al. (1976) observed ion–cyclotron waves in a quiescent plasma in which a low-energy beam of sodium ions was injected. A complete description of experimental results of electrostatic plasma oscillations near the ion–cyclotron frequency has been given by Motley and D'Angelo (1963). Several subsequent measurements of EIC oscillations and related phenomena were made under almost the same configuration and the results were discussed on the basis of current-driven instability (Hendel and Yamada 1974; Correl et al. 1975; Schrittwieser et al. 1984).

More recently, there has been a great deal of interest in studying EIC waves in multi-component plasmas (D'Angelo and Merlino 1986; Song et al. 1989; Suszcynsky et al. 1989; D'Angelo 1990; Barkan et al. 1995; Chow and Rosenberg 1995; Chow and Rosenberg 1996; Shukla and Mamun 2002; Shukla et al. 2009; Rosenberg 2010; Sharma and Sharma 2010a, b). Sharma et al. (2010) studied the excitation of ion–cyclotron waves by an ion beam in two-ion-component plasma. There have been a number of theoretical and experimental studies of EIC waves in negative ion plasmas. D'Angelo and Merlino (1986) analyzed EIC wave modes in plasma consisting of positive and negative ions and electrons. The EIC waves in plasma containing negative iodine ions were observed by Sheehan (1987). Song et al. (1989) studied EIC waves in a plasma with negative ions in a Q machine, and the results indicate that the frequencies of two EIC wave modes increase with the relative density of negative ions ε ($= n_{SF_6^-}/n_{k^+}$, where $n_{SF_6^-}$ is the density of sulfur hexafluoride ions and n_{k^+} is the density of potassium ions), while the critical electron drift velocities for the excitation of either mode decrease with increasing ε. Excitations of EIC waves in negative ion plasma by a magnetic field-aligned electron drift were also derived by Chow and Rosenberg (1996) using kinetic theory. They showed that the critical electron drift velocity for the excitation of both positive and negative ion modes decreased as the relative density of the negative ions increased. Experimental and theoretical investigations of EIC wave excitation in plasma containing negatively charged dust particles were performed by Barkan et al. (1995) and Chow and Rosenberg (1995)

Kim et al. (2008) studied EIC waves in a plasma with heavy negative ions where the excitation of fundamental

and higher harmonic light and heavy ion EIC modes were observed.

Rosenberg and Merlino (2009) presented a kinetic theory analysis of EIC instability in a plasma containing electrons and positive and negative ions. In this case, they investigated for exciting the fundamental and higher harmonic EIC waves associated with each ion species.

In this paper we study the generation of higher harmonics by a spiraling ion beam in a collisionless magnetized plasma containing two ion species (K^+ light positive ions and $C_7F_{14}^-$ heavy negative ions). The expression for growth rate for two unstable modes ($C_7F_{14}^-$ and K^+) is obtained in Sec. 2, using the first-order perturbation technique. Results and discussions are given in Sec. 3. Finally, the conclusions are given in Sec. 4.

2. Instability analysis

Consider a cylindrical plasma column of radius a_1 (containing K^+ light positive ions, $C_7F_{14}^-$ heavy negative ions, and electrons) with electron, positive ion, and heavy negative ion densities as $n_{e0} = (1-\varepsilon)n_{p0}$, $n_{+0} = n_{p0}$, and $n_{-0} = \varepsilon n_{p0}$, where ε ($= n_{C_7F_{14}^-}/n_{k^+}$, where $n_{C_7F_{14}^-}$ and n_{k^+} are the equilibrium densities of perfluoromethylcyclohexane and potassium ions respectively), n_{p0} is the plasma density, T_e is the temperature of electrons, $T_{k+}(= T_e)$ is the temperature of positive ions, and $_{TC_7F_{14}^-}(= T_e)$ is the temperature of heavy negative ions immersed in a uniform static magnetic field along z-axis. A spiraling ion beam of cesium with velocity $\overrightarrow{v_{b0}} \parallel \hat{z}$, mass m_b, density $n_{b0} = \frac{N_0\delta(r-r_b)}{2\pi r_b}$, and radius r_b propagates through the plasma along the magnetic field, where radius $r_b = \frac{v_{\theta 0}}{\omega_{cb}}$, where ω_{cb} is the beam cyclotron frequency and N_0 is the number of beam ions per unit axial length.

The beam plasma system prior to the perturbation is quasi-neutral such that $-n_{e0} - n_{-0} + n_{b0} + n_{+0} \approx 0$, since we have taken $n_{p0} \gg n_{b0}$. All the three species (electrons, heavy negative ions, and light positive ions) are treated as fluids, described by the equations of motion and continuity.

The equilibrium is perturbed by an electrostatic perturbation to the potential

$$\phi_1 = \phi(r)e^{-i(\omega t - l\theta - k_z Z)}. \tag{1}$$

The response of plasma electrons to the perturbation is governed by the equation of motion, which on linearization yields the perturbed velocity,

$$v_{\perp 1} = \frac{e}{m_e}\left[\frac{\nabla_\perp\phi \times \vec{\omega}_{ce} + i\omega\nabla_\perp\phi}{(\omega^2 - \omega_{ce}^2)}\right] - \frac{Te}{m_e n_{e0}}\frac{(i\omega\nabla_\perp n_{e1} + \nabla_\perp n_{e1} \times \vec{\omega}_{ce})}{(\omega^2 - \omega_{ce}^2)}, \tag{2}$$

$$v_{z1} = -\frac{ek_z\phi}{m_e\omega} + \frac{T_e k_z n_{e1}}{m_e\omega n_{e0}}, \tag{3}$$

where $\omega_{ce} = \frac{eB_s}{m_e c}$ is the electron–cyclotron frequency and subscript 1 refers to perturbed quantities. Substituting the perturbed velocities given by (2) and (3) in the mass conservation equation, we obtain the perturbed electron density as

$$n_{e1} = (1-\varepsilon)n_{p0}\frac{e\phi}{m_e v_{te}^2}, \tag{4}$$

where $v_{te}[= (T_e/m_e)^{1/2}]$ is the electron thermal velocity.

The response of positive ions is given by

$$\left(1 - \frac{C_+^2 k_z^2}{\omega^2}\right)n_{1+} + \frac{C_+^2\nabla_\perp^2 n_{1+}}{(\omega^2 - \omega_{c+}^2)} = -\frac{en_{+0}}{m_+}\left[\frac{\nabla_\perp^2\phi_1}{\omega^2 - \omega_{c_+^2}} - \frac{k_z^2\phi_1}{\omega^2}\right], \tag{5}$$

where C_+ $[= (T_e/m_+)^{1/2}]$ is the thermal velocity of positive ions and ω_{c+} $(= eB_s/m_+c)$, e, and m_+ are the cyclotron frequency, charge, and mass for positive ions respectively.

In the limit $\omega \sim \omega_{c+}$ and $\omega - \omega_{c+} > k_\perp C_+$, (5) gives the perturbed density for positive ions,

$$n_{1+} = -\frac{n_{p0}eC_+^2}{T_+}\left[\frac{\nabla_\perp^2\phi_1}{(\omega^2 - \omega_{c+}^2)} - \frac{k_z^2\phi_1}{\omega^2}\right]. \tag{6}$$

For heavy negative ions, by replacing e, m_+,ω_{C+}, T_+, and C_+ by $-$e, m_-,ω_{C-}, T_-, and C_- respectively in (5), we get

$$\left(1 - \frac{C_-^2 k_z^2}{\omega^2}\right)n_{1-} + \frac{C_-^2\nabla_\perp^2 n_{1-}}{(\omega^2 - \omega_{c-}^2)} = \frac{e\ n_{-0}}{m_-}\left[\frac{\nabla_\perp^2\phi_1}{\omega^2 - \omega_{c_-^2}} - \frac{k_z^2\phi_1}{\omega^2}\right]. \tag{7}$$

In the limit $\omega \sim \omega_{c-}$ and $\omega - \omega_{c-} > k_\perp c_-$ ($|k_\perp\rho_h| < 1$), $\rho_h(= C_-/\omega_{c-})$ is the heavy ion larmor radius, i.e., if heavy ion larmor radius is less than the perpendicular wavelength of the mode, then (7) gives the perturbed density for heavy negative ions (in the limit of strongly magnetized plasma),

$$n_{1-} = \frac{n_{p0}e \in C_-^2}{T_e}\left[\frac{\nabla_\perp^2\phi_1}{\omega^2 - \omega_{c-}^2} - \frac{k_z^2\phi_1}{\omega^2}\right], \tag{8}$$

where $C_-[= (T_e/m_-)^{1/2}]$ is the thermal velocity of heavy negative ions and $\omega_{c-}(= e\ B_s/m_-c)$ is the cyclotron frequency of heavy negative ions. By following Sharma and Tripathi (1993), the perturbed ion beam density can be written as

$$n_{b1} = \frac{N_0\delta(r-r_b)}{(\omega_1 - l\omega_{cb})^2}\frac{e}{m_b}\frac{\left(\frac{l^2}{r^2} + K_z^2\right)\phi_1}{2\pi r_b}, \tag{9}$$

where $\omega_1 = \omega - k_z v_{b0}$.

Using (4), (6), (8), and (9) in Poisson's equation $\nabla^2\phi_1 = 4\pi e(-n_{1+} - n_{1b} + n_{e1} + n_{1-})$, we obtain a second-order differential equation in ϕ_1, which can be rewritten for

https://doi.org/10.1017/S002237781300007X Published online by Cambridge University Press

axially symmetric case as

$$\frac{\partial^2\phi_1}{\partial r^2}+\frac{1}{r}\frac{\partial\phi_1}{\partial r}+\left(p^2-\frac{l^2}{r^2}\right)\phi_1 = -\frac{2N_0e^2\left(\frac{l^2}{r^2}+K_z^2\right)\phi_1\delta(r-r_b)}{m_b(\omega_1-l\omega_{cb})^2r_bL}, \quad (10)$$

where

$$p^2=\frac{\frac{\omega_{pl}^2k_z^2}{\omega^2}+\frac{\omega_{ph}^2k_z^2}{\omega^2}-\frac{\omega_{pe}^2}{v_{te}^2}-k_z^2}{1-\frac{\omega_{pl}^2}{\omega^2-\omega_{c+}^2}-\frac{\omega_{ph}^2}{\omega^2-\omega_{c-}^2}}, \quad (11)$$

$$L=1-\frac{\omega_{pl}^2}{\omega^2-\omega_{c+}^2}-\frac{\omega_{ph}^2}{\omega^2-\omega_{c-}^2},$$

$$\omega_{pe}^2=\frac{4\pi\ n_{e0}e^2}{m_e},\omega_{ph}^2=\frac{4\pi\ \varepsilon n_{p0}e^2}{m_-},$$

and $\omega_{pl}^2=\frac{4\pi\ n_{p0}e^2}{m_+}$.

In the absence of the beam, when the right-hand side (RHS) is zero, the solution of (10) is given by $\phi_1=AJ_l(p_n r), p_1=p_n$. At $r=a_1$, ϕ_1 must vanish, hence $J_l(p_na_1)=0$, i.e., $p_n=\frac{x_n}{a_1}\quad(n=1,2,\ldots),\quad x_n$ are the zeros of the Bessel function $J_l(x)$. In the presence of the beam, the solution wave function ϕ_1 can be expressed in a series of orthogonal sets of wave functions:

$$\phi_1=\sum\nolimits_m A_mJ_l(p_mr). \quad (12)$$

Now substituting the value of ϕ_1 from (12) in (10), we multiply both sides of (10) by $rJ_l(p_nr)$ and integrating over r from 0 to a_1 (where a_1 is the plasma radius), we get

$$p^2-p_n^2=-\frac{\Omega_{pb}^2\left(\frac{l^2}{r_b^2}+k_z^2\right)J_l^2(p_nr_b)}{L(\omega_1-l\omega_{cb})^2J_{l+1}^2(p_na_1)}. \quad (13)$$

Substituting the value of p^2 from (11) into (13), we obtain

$$1-\frac{\omega_{pl}^2k_z^2}{p_n^2\alpha\omega^2}-\frac{\omega_{ph}^2}{\omega^2}\frac{k_z^2}{p_n^2\alpha}-\frac{\omega_{pl}^2}{(\omega^2-\omega_{c+}^2)\alpha}-\frac{\omega_{ph}^2}{(\omega^2-\omega_{c-}^2)\alpha} = -\frac{\Omega_{\mathrm{pb}}^2\left(\frac{l^2}{r_b^2}+k_z^2\right)J_l^2(p_nr_b)}{p_n^2\alpha(\omega_1-l\omega_{cb})^2J_{l+1}^2(p_na_1)}, \quad (14)$$

where $\Omega_{pb}^2=\frac{4N_0e^2}{m_ba_1^2}$,

$$\alpha=\frac{p_n^2+k_z^2}{p_n^2}+\frac{\omega_{pe}^2}{v_{te}^2p_n^2}=1+\frac{\omega_{pi}^2}{C_s^2p_n^2}\cong\frac{\omega_{pi}^2}{C_s^2p_n^2}\text{ and }C_s^2=\frac{T_e}{m_i}.$$

2.1. Beam plasma interaction with light positive (K^+) ions

In the absence of heavy negative ions (i.e., in the limit $\omega\sim\omega_{c+}$, and light ion Larmor radius is less than the perpendicular wavelength of the mode), (14) can be rewritten as:

$$1-\frac{\omega_{pl}^2k_z^2}{p_n^2\alpha\omega^2}-\frac{\omega_{pl}^2}{(\omega^2-\omega_{c+}^2)\alpha} = -\frac{\Omega_{pb}^2\left(\frac{l^2}{r_b^2}+k_z^2\right)J_l^2(p_nr_b)}{p_n^2\alpha(\omega_1-l\omega_{cb})^2J_{l+1}^2(p_na_1)}. \quad (15)$$

Equation (15) can be rewritten as

$$(\omega^2-c_1^2)(\omega^2-c_2^2)(\omega-k_zv_{b0}-l\omega_{cb})^2 = \frac{\omega^2(\omega^2-\omega_{c+}^2)\Omega_{pb}^2\left(\frac{l^2}{r_b^2}+k_z^2\right)J_l^2(p_nr_b)}{p_n^2\alpha J_{l+1}^2(p_na_1)}, \quad (16)$$

where

$$\omega^2=c_1^2=\omega_{c+}^2+(k_z^2+p_n^2)C_s^2\frac{1}{(1-\varepsilon)}, \quad (17)$$

$$\omega^2=c_2^2=\frac{\omega_{c+}^2\frac{1}{1-\varepsilon}k_z^2C_S^2}{\omega_{c+}^2+\frac{1}{1-\varepsilon}k^2C_S^2}, \quad (18)$$

and $k^2=p_n^2+k_z^2$, $p_n^2>k_z^2$. Here $\omega\cong c_1$, $\omega\cong k_zv_{b0}+l\omega_{cb}$ corresponding to the dispersion relation of the EIC wave and the beam mode respectively. In (18) if we take $\varepsilon=0$, then we can recover the dispersion relation of Sharma and Tripathi (1993). When $n_{b0}\neq0$, we can expand it as

$$\omega=c_1+\delta_1=k_zv_{bo}+l\omega_{cb}+\delta_1,$$

where δ_1 is the modification in ω due to the finite RHS of (16).

Thus, (16) gives the growth rate of the unstable (light positive ion) mode,

$$\gamma=\mathrm{Im}\ \delta_1 = \frac{\sqrt{3}}{2}\left[\frac{c_1(c_1^2-\omega_{c+}^2)\Omega_{pb}^2\left(\frac{l^2}{r_b^2}+k_z^2\right)J_l^2(p_nr_b)}{2(c_1^2-c_2^2)p_n^2\left[\frac{p_n^2+k_z^2}{p_n^2}+\frac{\omega_{pi}^2}{C_s^2p_n^2}\right]J_{l+1}^2(p_na_1)}\right]^{1/3}. \quad (19)$$

The real part of the frequency of the unstable mode for light positive ions in terms of beam energy is given as

$$\omega_r=k_z(2eV_b/m)^{1/2} -\frac{1}{2}\left[\frac{c_1(c_1^2-\omega_{c+}^2)\Omega_{pb}^2\left(\frac{l^2}{r_b^2}+k_z^2\right)J_l^2(p_nr_b)}{2(c_1^2-c_2^2)p_n^2\left[\frac{p_n^2+k_z^2}{p_n^2}+\frac{\omega_{pi}^2}{C_s^2p_n^2}\right]J_{l+1}^2(p_na_1)}\right]^{1/3}. \quad (20)$$

https://doi.org/10.1017/S002237781300007X Published online by Cambridge University Press

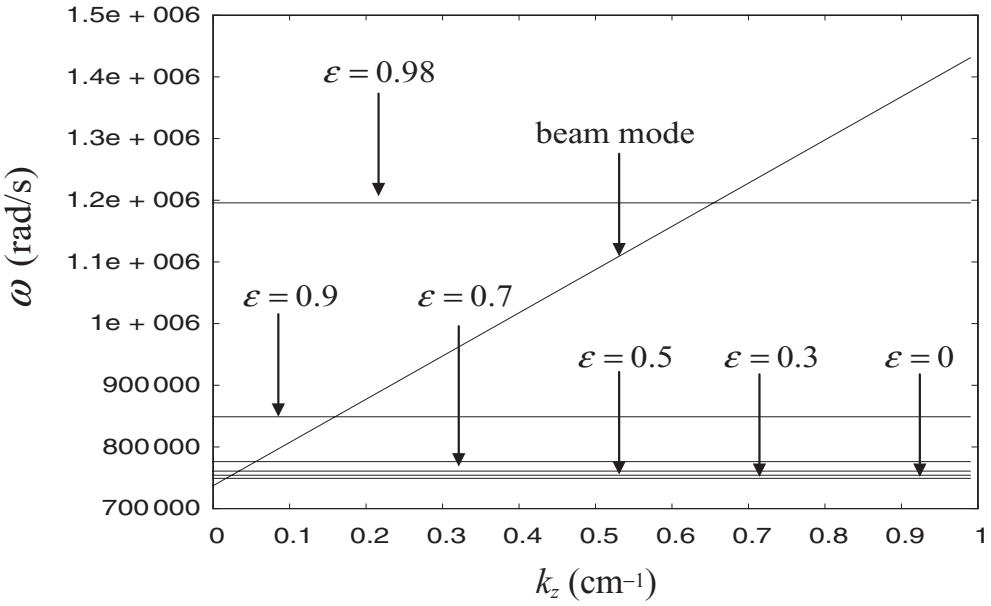

Figure 1. Dispersion curves of EIC waves with light positive ions and a beam mode for different values of ε. The parameters are given in the text.

2.2. *Beam plasma interaction with heavy negative ($C_7F_{14}^-$) ions*

In the absence of positive ions (i.e., in the limit $\omega \sim \omega_{c-}$, and heavy ion Larmor radius is less than the perpendicular wavelength of the mode), (14) can be rewritten as

$$1-\frac{\omega_{ph}^2 k_z^2}{p_n^2\alpha\omega^2}-\frac{\omega_{ph}^2}{\left(\omega^2-\omega_{c-}^2\right)\alpha}=-\frac{\Omega_{pb}^2\left(\frac{l^2}{r_b^2}+k_z^2\right)J_l^2(p_n r_b)}{p_n^2\alpha(\omega_1-l\omega_{cb})^2 J_{l+1}^2(p_n a_1)}. \tag{21}$$

Equation (21) can be rewritten as

$$\left(\omega^2-d_1^2\right)\left(\omega^2-d_2^2\right)(\omega-k_z v_{b0}-l\omega_{cb})^2 = \frac{\omega^2\left(\omega^2-\omega_{c-}^2\right)\Omega_{pb}^2\left(\frac{l^2}{r_b^2}+k_z^2\right)J_l^2(p_n r_b)}{p_n^2\alpha J_{l+1}^2(p_n a_1)}, \tag{22}$$

where

$$d_1^2=\omega_{c-}^2+\frac{\varepsilon}{(1-\varepsilon)}\left(k_z^2+p_n^2\right)C_s^2\frac{m_i}{m_-} \text{ and} \tag{23}$$

$$d_2^2=\frac{\omega_{c-}^2\frac{\varepsilon}{1-\varepsilon}k_z^2C_S^2\frac{m_i}{m_-}}{\omega_{c-}^2+\frac{\varepsilon}{1-\varepsilon}\frac{m_i}{m_-}k^2C_S^2}. \tag{24}$$

If we assume $n_{-0} = n_{p0}$, then in (23) and (24) the parameter $\varepsilon/1-\varepsilon$ is replaced by $1/1-\varepsilon$. In the absence of negative ions, i.e., $\varepsilon = 0$ and for equal masses of ions, i.e., positive ion mass = negative ion mass, from (23) and (24), we can recover the dispersion relation of ion cyclotron waves of Sharma and Tripathi (1993).

By following the earlier method, (22) gives the growth rate of the unstable (heavy negative ion) mode,

$$\gamma=\frac{\sqrt{3}}{2}\left[\frac{d_1\left(d_1^2-\omega_{c-}^2\right)\Omega_{pb}^2\left(\frac{l^2}{r_b^2}+k_z^2\right)J_l^2(p_n r_b)}{2\left(d_1^2-d_2^2\right)p_n^2\left[\frac{p_n^2+k_z^2}{p_n^2}+\frac{\omega_{pi}^2}{C_s^2p_n^2}\right]J_{l+1}^2(p_n a_1)}\right]^{1/3}. \tag{25}$$

The real part of the frequency of the unstable heavy negative ion mode in terms of beam energy is given as

$$\omega_r=k_z(2eV_b/m)^{1/2}$$

$$-\frac{1}{2}\left[\frac{d_1\left(d_1^2-\omega_{c+}^2\right)\Omega_{pb}^2\left(\frac{l^2}{r_b^2}+k_z^2\right)J_l^2(p_n r_b)}{2\left(d_1^2-d_2^2\right)p_n^2\left[\frac{p_n^2+k_z^2}{p_n^2}+\frac{\omega_{pi}^2}{C_s^2p_n^2}\right]J_{l+1}^2(p_n a_1)}\right]^{1/3} \tag{26}$$

3. Results and discussions

We have used typical negative ion plasma parameters in our calculations. In Figs. 1 and 2, we have plotted the dispersion curves of an ion–cyclotron wave for the following parameters: electron plasma density $n_{e0} = 10^9 \text{cm}^{-3}$, electron and ion temperatures are assumed to be $T_e = T_i = 0.2$ eV, plasma radius $a_1 = 2$ cm, magnetic field $B_s = 0.5$ kg, the relative density of heavy negative ions, i.e., $\varepsilon (= n_{C_7F_{14}^-}/n_{K^+}$, where $n_{C_7F_{14}^-}$ and n_{K^+} are the equilibrium densities of perfluoromethylcyclohexane and potassium ions respectively) 0–0.98. We have also plotted the beam mode for the beam energy $E_b = 10$ eV (cf. Figs. 1 and 2). The frequencies and the corresponding

https://doi.org/10.1017/S002237781300007X Published online by Cambridge University Press

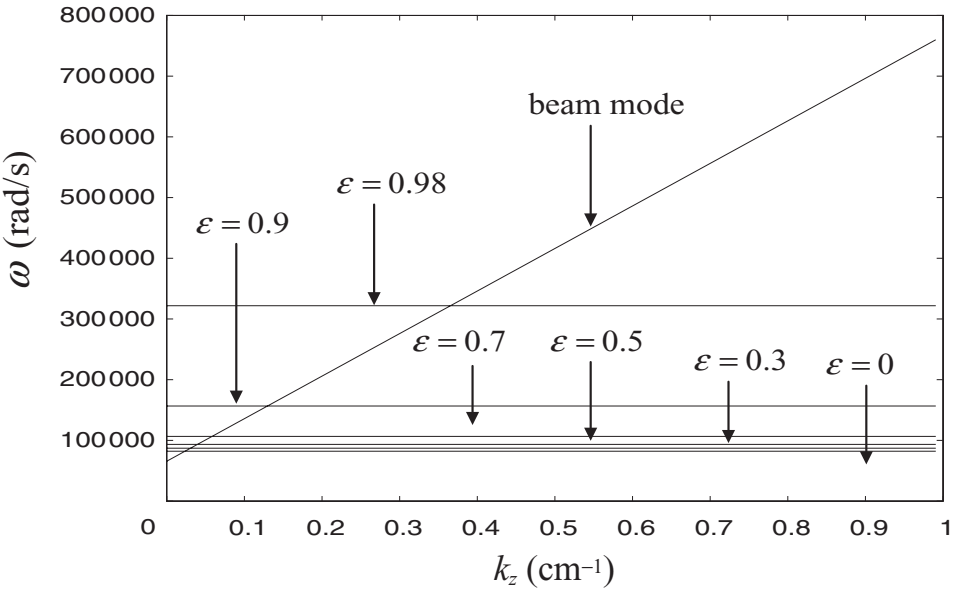

Figure 2. Dispersion curves of EIC waves with heavy negative ions and a beam mode for different values of ε. The parameters are given in the text.

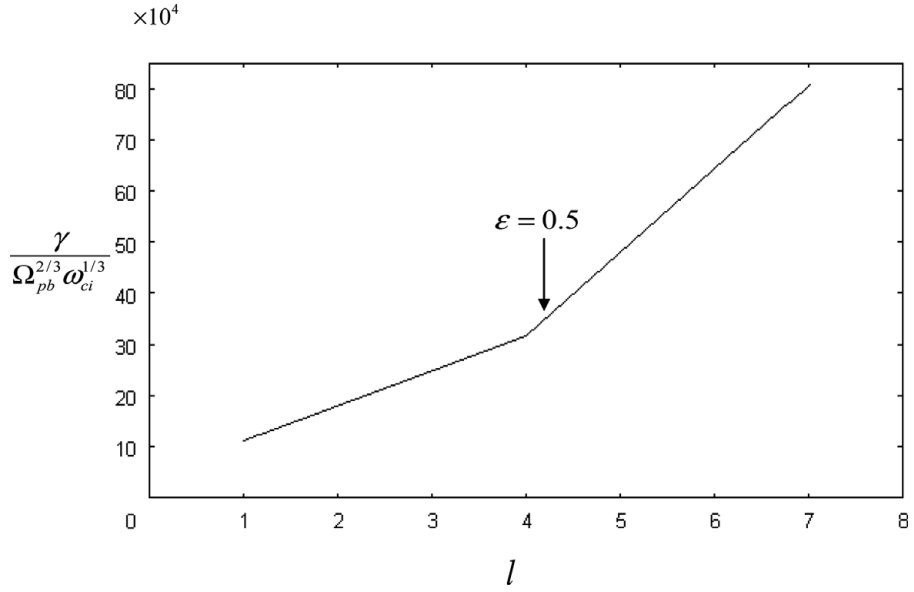

Figure 3. Normalized growth rates of light positive ion mode as a function of the azimuthal mode ℓ for $\varepsilon = 0.5$ for the same parameters as in Fig. 1 and for beam density $n_{bo} = 4 \times 10^6$ cm^{-3} and beam radius $r_b = 1.5$ cm.

wave numbers of the unstable wave are obtained by the point of intersections between the beam mode and plasma mode, and are given in Tables 1 and 2. It can be seen from Figs. 1 and 2 that the positive ion mode is a higher frequency mode and the heavy negative ion mode is a lower frequency mode. It can also be seen that as the negative ion density increases, the unstable frequencies of both the modes also increases (cf. Figs. 1 and 2).

Using (19) and (25), we plotted in Figs. 3 and 4 the normalized growth rate γ of the two unstable modes versus the azimuthal mode number ℓ for the same parameters as used for plotting Figs. 1 and 2 and for beam density $n_{b0} = 4 \times 10^6 \text{cm}^{-3}$ and beam radius $r_b = 1.5$ cm. From Figs. 3 and 4, it can be seen that the growth rates of both unstable modes increase with the azimuthal mode number ℓ. The growth rate

Table 1. From Fig. 1 (ion beam + plasma with light positive ions) we obtain the values of unstable wave frequencies ω (rad/s) and axial wave numbers k_z (cm^{-1}) for different values of $\varepsilon = 0$, 0.3, 0.5, 0.7, 0.9, and 0.98 and $\ell = 1$.

ε	k_z(cm^{-1})	ω (rad/s)
0	0.0150	7.509×10^5
0.3	0.0200	7.550×10^5
0.5	0.0332	7.633×10^5
0.7	0.0547	7.776×10^5
0.9	0.1571	8.496×10^5
0.98	0.6525	1.192×10^6

https://doi.org/10.1017/S002237781300007X Published online by Cambridge University Press

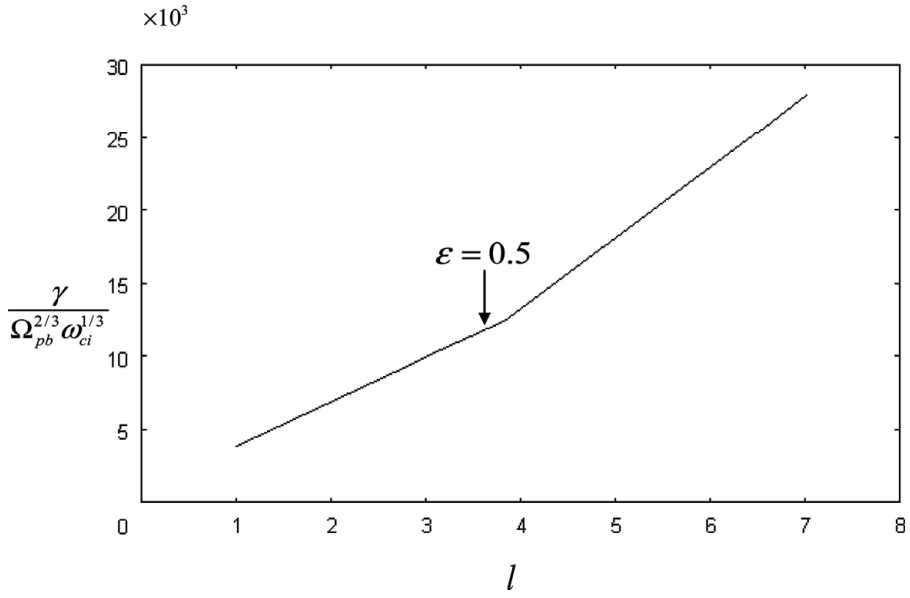

Figure 4. Normalized growth rates of the heavy negative ion mode as a function of the azimuthal mode ℓ for $\varepsilon = 0.5$ for the same parameters as in Fig. 2 and for beam density $n_{bo} = 4 \times 10^6$ cm^{-3} and beam radius $r_b = 1.5$ cm.

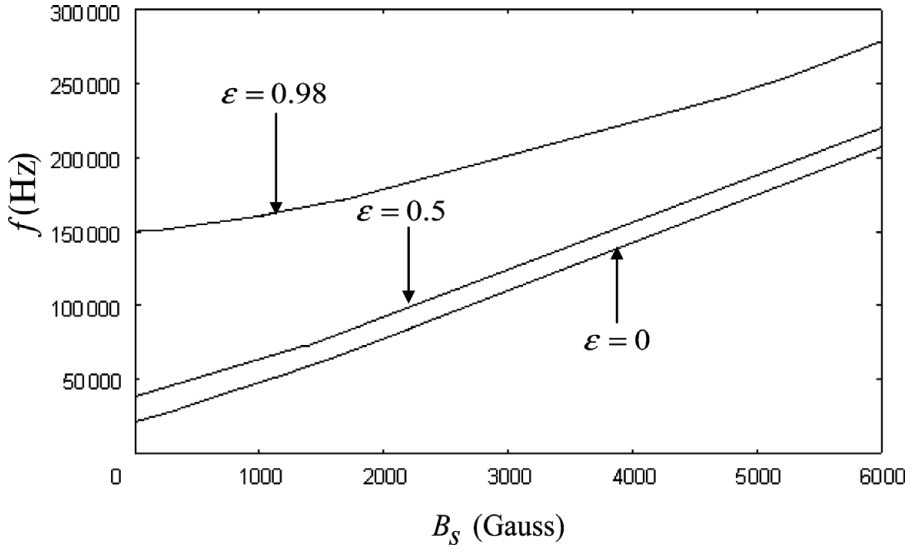

Figure 5. Frequency f ($= \omega_r/2\pi$ in Hz) of the unstable mode for light positive ions as a function of magnetic field B_s (in gauss) for different values of relative density of heavy negative ions ε.

Table 2. From Fig. 2 (ion beam + plasma with heavy negative ions) we obtain the values of unstable wave frequencies ω (rad/s) and axial wave numbers k_z (cm^{-1}) for $\varepsilon = 0$, 0.3, 0.5, 0.7, 0.9, and 0.98 and $\ell = 1$.

ε	k_z(cm^{-1})	ω (rad/s)
0	0.02140	8.376×10^4
0.3	0.03097	8.914×10^4
0.5	0.03896	9.633×10^4
0.7	0.05814	1.088×10^5
0.9	0.12687	1.573×10^5
0.98	0.36498	3.224×10^5

increases up to $\ell = 6$ and becomes maximum at $\ell = 7$. These results of growth rates are consistent with the theoretical predictions of Sharma and Tripathi (1993). If we compare Figs. 3 and 4 with Fig. 1 of Sharma and Tripathi (1993), the trend of our plots seems to be consistent with theoretical predictions.

The growth rates of both unstable modes in presence of K^+ and $C_7F_{14}^-$ ions increase with beam density and scales as the one-third power of the beam density (cf. (19) and (25)). It can be seen from Figs. 5 and 6 that the frequency of both unstable modes increases with increasing magnetic fields and this increase in frequency is linear. We have also plotted frequency versus relative density of negative ions ε of both unstable modes and found that the frequency f (in Hz) increases with ε for different values of magnetic fields B_s (in Tesla). It can also be seen from Figs. 7 and 8 that for $\varepsilon \leqslant 0.6$, the increase in frequency is not so significant but as the relative density of negative ions increases further,

https://doi.org/10.1017/S002237781300007X Published online by Cambridge University Press

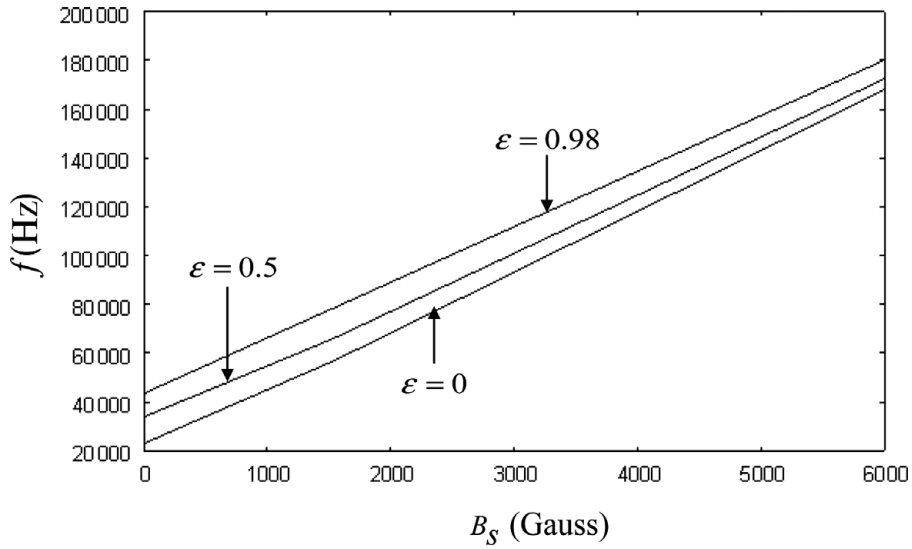

Figure 6. Frequency f ($= \omega_r/2\pi$ in Hz) of the unstable mode for heavy negative ions as a function of the magnetic field B_s (in gauss) for different values of relative density of heavy negative ions ε.

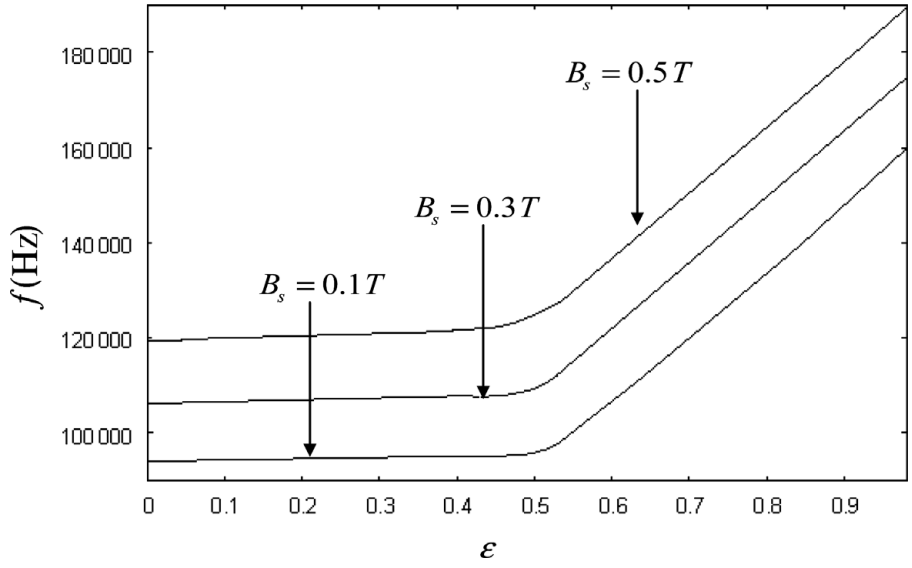

Figure 7. Frequency f ($= \omega_r/2\pi$ in Hz) of the unstable light positive ion mode as a function of ε for different values of magnetic field strength B_s (in Tesla).

i.e., for $\varepsilon \geqslant 0.6$, unstable frequencies of both unstable modes increase and become maximum at 0.98 (cf. Figs. 7 and 8). The real part of frequency of unstable modes increases with beam energy and scales as almost the one-half power of the beam energy (cf. (20) and (26)). At $\omega \approx \omega_{ci}$, the ion–cyclotron mode is strongly cyclotron damped on plasma ions and hence cannot be driven. For $\omega - \omega_{ci} \gg k_z v_{ti}$, collisionless cyclotron damping is weak and the growth rate scales as the cube root of the beam current. In the present case, we have chosen the parameters in such a way that the collisionless damping does not play any significant role. Moreover, we have shown that by increasing the relative density of heavy negative ions, the growth rate of unstable mode increases. This result is in line of Song et al. (1989), where it was shown that the critical electron drift for the excitation of either mode (positive or negative ion) decreases as the density of negative ions increases.

In the present calculations plasma radius $a_1 = 2$ cm and spiraling ion beam radius $r_b = 1.5$ cm. For the parameters mentioned in the manuscript, beam radius $\gg$ the gyroradius of ion beam ρ_L or ρ_h ($= \frac{c_+}{\omega_{c+}}$ or $\frac{c-}{\omega_{c-}}$). Hence the ion beam will spiral in a device.

4. Conclusion

In conclusion, we may say that a spiraling ion beam propagating through a magnetized plasma cylinder drives ion–cyclotron waves to instability when ion beam possesses a large perpendicular energy. The presence of heavy negative ions in plasma has a significant effect on the excitation of light positive ion and heavy negative ion

https://doi.org/10.1017/S002237781300007X Published online by Cambridge University Press

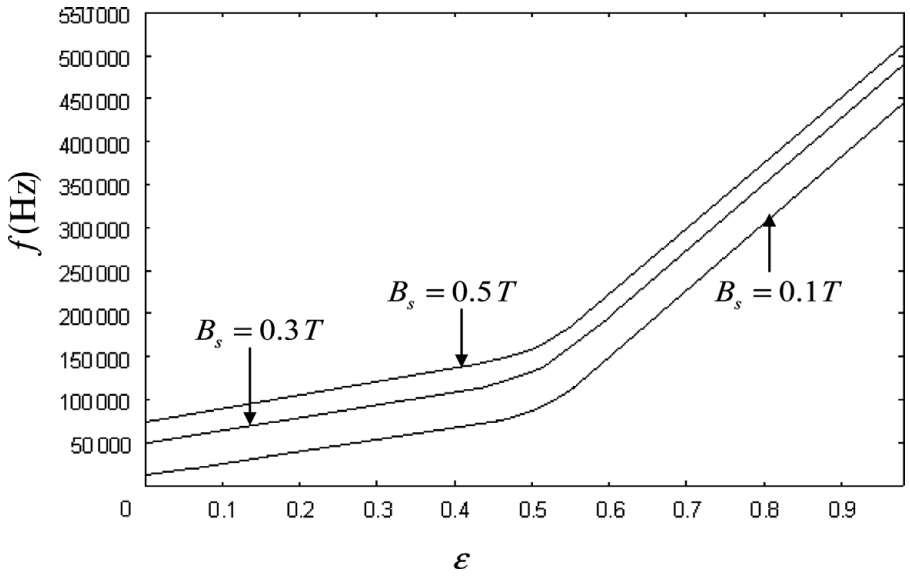

Figure 8. Frequency f ($= \omega_r/2\pi$ in Hz) of the unstable heavy negative ion mode as a function of ε for different values of magnetic field strength B_s (in Tesla).

EIC wave modes. The frequency of both unstable modes is less than the ion–cyclotron frequency, and it increases with the azimuthal mode numbers slightly more rapidly than linear. The growth rates and mode frequencies are evaluated for typical negative ion plasma parameters, and it is found that the unstable mode frequencies increase with the relative density of negative ions. The growth rate of unstable modes has the largest value for the modes whose eigen functions peak at the location of the beam.

Our theoretical predictions, e.g., mode frequencies versus relative density of light positive and heavy negative ions, mode frequencies versus magnetic fields for different relative densities of light positive and heavy negative ions, and mode frequencies versus relative density of light positive and heavy negative ions for different values of magnetic fields are in line with the experimental observations (cf. Song et al. 1989; Kim et al. 2008) and theoretical results (cf. D'Angelo and Merlino 1986; Chow and Rosenberg 1996). In addition, our theoretical predictions of higher harmonic generation results are also in line with the experimental observations of Kim et al. (2008) and theoretical predictions of Kim et al. (2008) and Rosenberg and Merlino (2009). However, we cannot compare our theoretical results with the experiments that do not have spiraling ion beams.

Our theoretical model is useful in predicting the excitation of higher harmonic EIC wave modes by a spiraling ion beam and the dependence of mode frequencies on the relative density of negative ions. Negative ions have been found in ionospheres of Mercury, Earth's Moon, and Jupiter's Moon as well as in stellar atmospheres, so this model may find applications in such situations (Horwitz 1982; Coates et al. 2007). Ion–cyclotron waves are extremely useful in plasma heating devices. In this case, the electrons move with velocity close to the phase velocity of the wave, resonantly absorbing energy from the wave via Cerenkov interaction.

References

Barkan, A., D'Angelo, N. and Merlino, R. L. 1995 *Planet. Space Sci.* **43**, 905.

Bergman, R. 1984 *J. Geophys. Res.* **89**, 953.

Chow, V. W. and Rosenberg, M. 1995 *Planet. Space Sci.* **43**, 613.

Chow, V. W. and Rosenberg, M. 1996 *Plasma Phys.* **3**, 1202.

Coates, A. J., Crary, F. J., Lewis, G. R., Young, D. T., Waiter, Jr. J. H., Sittler, Jr. E. C. 2007a *Geophys. Res. Lett.* **34**, L22103.

Correl, D. L., Rynn, N. and Bohmer, H. 1975 *Phys. Fluids* **18**, 1800.

D'Angelo, N. 1973 *J. Geophys. Res.* **78**, 3987.

D'Angelo, N. 1990 *Planet. Space Sci.* **38**, 1143.

D'Angelo, N. and Merlino, R. L. 1986 *IEEE Trans. Plasma Sci.* **PS-14**, 285.

D'Angelo, N. and Motley, R. W. 1962 *Phys. Fluids* **5**, 633.

Drummoned, W. E. and Rosenbluth, M. N. 1962 *Phys. Fluids* **5**, 1507.

Hendel, H. W. and Yamada, M. 1974 *Phys. Rev. Lett.* **33**, 1076.

Horwitz, J. L. 1982 *Rev. Geophys.* **29**, 929.

Ishizuka, H., Ono, H. and Kojima, S. 1974 *J. Phys. Soc. Japan* **36**, 1158.

Kim, S. H., Heinrich, J. R. and Merlino, R. L. 2008 *Planet. Space Sci.* **56**, 1552.

Michelson, P., Pecseli, H. L., Ramussen, J. J. and Sato, N. 1976 *Phys. Fluids* **19**, 453.

Motley, R. W. and D'Angelo, N. 1963 *Phys. Fluids* **6**, 296.

Rosenberg, M. 2010 *Phys. Scr.* **82**, 3.

Rosenberg, M. and Merlino, R. L. 2009 *J. Plasma Physics* **75**, 495.

Schrittwieser, R., Rynn, R., Koslover, R., and Karim, R. 1984 *Plasma Phys. Control. Fusion* **26**, 1597.

https://doi.org/10.1017/S002237781300007X Published online by Cambridge University Press

Sharma, J. and Sharma, S. C. 2010a *Phys. Plasmas* **17**, 123701.
Sharma, S. C. and Sharma, J. 2010b *Phys. Plasmas* **17**, 043704.
Sharma, S. C. and Tripathi, V. K. 1993 *J. Plasma Physics* **50**, 331.
Shukla, P. K. and Mamun, A. A. 2002 *Introduction to Dusty Plasma Physics*. Bristol, UK: IOP.
Shukla, P. K. and Eliasson, B. 2009 *Rev. Mod. Phys.* **81**, 25.
Song, B., Suszcynsky, D., D'Angelo, N. and Merlino, R. L. 1989 *Phys. Fluids* B **1**, 2316.
Suszcynsky, D. M., D'Angelo, N. and Merlino, R. L. 1989 *J. Geophys. Res.* **94**, 8966.

https://doi.org/10.1017/S002237781300007X Published online by Cambridge University Press